Author/s:
Bernardo, BC;Ooi, JYY;Matsumoto, A;Tham, YK;Singla, S;Kiriazis, H;Patterson, NL;Sadoshima, J;Obad, S;Lin, RCY;McMullen, JR

Title:
Sex differences in response to miRNA-34a therapy in mouse models of cardiac disease: identification of sex-, disease- and treatment-regulated miRNAs

Date:
2016-10-15

Citation:
Bernardo, B. C., Ooi, J. Y. Y., Matsumoto, A., Tham, Y. K., Singla, S., Kiriazis, H., Patterson, N. L., Sadoshima, J., Obad, S., Lin, R. C. Y. & McMullen, J. R. (2016). Sex differences in response to miRNA-34a therapy in mouse models of cardiac disease: identification of sex-, disease- and treatment-regulated miRNAs. Journal of Physiology, 594 (20), pp.5959-5974. https://doi.org/10.1113/JP272512.

Sex differences in response to miRNA-34a therapy in mouse models of cardiac disease: Identification of sex-, disease- and treatment-regulated miRNAs

Bianca C. Bernardo[1*], Jenny Y.Y. Ooi[1], Aya Matsumoto[1], Yow Keat Tham[1,2], Saloni Singla[1], Helen Kiriazis[1], Natalie L. Patterson[1], Junichi Sadoshima[3], Susanna Obad[4], Ruby C. Y. Lin[5], Julie R. McMullen[1,2,6*]

[1]Baker IDI Heart and Diabetes Institute, Melbourne, VIC, 3004, Australia.
[2]Department of Medicine, Monash University, Clayton, VIC, 3004, Australia.
[3]Department of Cell Biology and Molecular Medicine, Rutgers New Jersey Medical School, The State University of New Jersey, Newark, New Jersey 07103, USA.
[4]Roche Innovation Center Copenhagen, Hørsholm, 2970, Denmark.
[5]Asbestos Diseases Research Institute, Concorde Hospital, Sydney, NSW, 2139, Australia.
[6]Department of Physiology, Monash University, Clayton, VIC, 3800, Australia.

*Address Correspondence to:
Julie R. McMullen
PO Box 6492, St Kilda Road Central
Melbourne 3004, Australia
Tel: +61 3 8532 1194
Fax: +613 8532 1100
E-mail: julie.mcmullen@bakeridi.edu.au

Bianca C. Bernardo
PO Box 6492, St Kilda Road Central
Melbourne 3004, Australia
Tel: +61 3 8532 1167
Fax: +613 8532 1100
E-mail: bianca.bernardo@bakeridi.edu.au

This is the author manuscript accepted for publication and has undergone full peer review but has not been through the copyediting, typesetting, pagination and proofreading process, which may lead to differences between this version and the Version of Record. Please cite this article as doi: 10.1113/JP272512.

Key points

- MiRNA-based therapies are in development for numerous diseases including heart disease. There is currently very limited basic information on the regulation of specific miRNAs in male and female hearts in settings of disease. The identification of sex-specific miRNA signatures has implications for translation into the clinic and suggests a need for customised therapy.
- In the present study, we found that a miRNA-based treatment inhibiting miR-34a was more effective in females in a setting of moderate dilated cardiomyopathy than males. Furthermore, the treatment showed little benefit in a setting of more severe dilated cardiomyopathy associated with atrial fibrillation, in either sex.
- The results have highlighted the importance of understanding the effect of miRNA-based therapies in cardiac disease settings in males and females.

Abstract

microRNA-34a (miR-34a) is elevated in the diseased heart in mice and humans. Previous studies have shown that inhibiting miR-34a in male mice in settings of pathological cardiac hypertrophy or ischemia protects the heart against progression to heart failure. Whether inhibition of miR-34a protects the female heart is unknown. Furthermore, the therapeutic potential of silencing miR-34a in settings of dilated cardiomyopathy (DCM) and atrial fibrillation (AF) had not previously been assessed. In the present study, we examined the effect of silencing miR-34a in males and females in 1) a model of moderate DCM and 2) a model of severe DCM with AF. The cardiac disease models were administered with a locked nucleic acid-modified oligonucleotide (LNA-antimiR-34a) at 6-7 weeks of age when the models display cardiac dysfunction and conduction abnormalities. Cardiac function and morphology were measured 6 weeks after treatment. Here, we show that inhibition of miR-34a provides more protection in the DCM model in females than males. Disease prevention in LNA-antimiR-34a treated DCM female mice was characterised by attenuated heart enlargement and lung congestion, lower expression of cardiac stress genes (B-type natriuretic peptide, collagen gene expression), less cardiac fibrosis and better cardiac function. There

was no evidence of significant protection in the severe DCM and AF model in either sex. Sex- and treatment-dependent regulation of miRNAs was also identified in the diseased heart, and may explain the differential response of males and females. These studies highlight the importance of examining the impact of miRNA-based drugs in both sexes and different disease conditions.

Summary statement: MiRNA-based therapies are in development for numerous diseases including heart disease. In this study, we found that a miRNA-based treatment targeting miR-34a was more effective in females than males in a setting of moderate dilated cardiomyopathy.

Running title: miR-34a and sex differences in cardiac disease

Keywords: microRNAs, heart failure, dilated cardiomyopathy, miR-34a, atrial fibrillation

Abbreviations: AF, atrial fibrillation; AW, atria weight; BNP, B-type natriuretic peptide; BW, body weight; DCM, dilated cardiomyopathy; dnPI3K, dominant negative phosphoinositide 3-kinase; ECG, electrocardiogram; ECHO, echocardiography; FS, fractional shortening; HR, heart rate; HW, heart weight; LNA, locked nucleic acid; LV, left ventricle/ventricular; LVEDD, LV end-diastolic dimension; LVESD, LV end-systolic dimension; LVPW, LV posterior wall thickness; LW, lung weight; MI, myocardial infarction; miRNA/miR, microRNA; Mst1, mammalian sterile 20-like kinase 1; Ntg, non-transgenic; PI3K, phosphoinositide 3-kinase; TL, tibia length.

INTRODUCTION

Sex differences in the incidence, prevalence, symptoms, age at onset, and severity of disease are now well documented in humans (Kim *et al.*, 2010; Legato, 2016). This is particularly evident in cardiovascular disease. In both animal and human studies, it is apparent that there are sex differences in the degree of cardiac pathology in response to cardiac insults such as pressure overload (see review (Bernardo *et al.*, 2010)). However, the molecular mechanisms underlying sex dimorphism are complex and are still not well understood. Data from clinical trials also demonstrates that males and females respond differently to cardiovascular drugs. For instance, conventional pharmacological therapies including angiotensin-converting enzyme inhibitors and beta-blockers are generally less effective in women than men, and show more side effects (Regitz-Zagrosek, 2006). Further, higher mortality has been reported in women treated with digoxin (Rathore *et al.*, 2002). Despite these differences, biomedical research continues to use many more male subjects than females in both animal studies and human clinical trials (Editorial, 2010; Legato, 2016).

MicroRNAs (miRNAs) are a class of non-coding RNAs that regulate gene expression by directing their target mRNAs for degradation or translational repression (Bernardo *et al.*, 2012a). MiRNAs are dysregulated in a number of disease settings, including cardiovascular disease (Hata, 2013). Targeting disease-induced miRNAs is considered a promising therapeutic approach, with a number of drugs being tested in clinical trials and/or being developed (Janssen *et al.*, 2013; Bernardo *et al.*, 2015). While sex differences are well recognised in human disease, relatively few studies have specifically examined miRNA sex differences in humans (Sharma & Eghbali, 2014). In the small number of human studies performed, sex-based expression of miRNAs has been identified in disorders including metabolic syndrome, schizophrenia, and cancer (Sharma & Eghbali, 2014). To date, the study of sex differences in miRNAs in humans with cardiovascular disease remains largely unexplored, and represents a key knowledge gap (Sharma & Eghbali, 2014).

A miRNA which has received particular interest in the heart is miR-34a. The expression of miR-34a is elevated in the mouse heart in a number of cardiac stress settings including pathological hypertrophy, ischemia due to myocardial infarction (MI), and ageing (Bernardo *et al.*, 2012b; Boon *et al.*, 2013; Bernardo *et al.*, 2014a; Huang *et al.*, 2014; Yang *et al.*, 2015). Of clinical relevance, expression of miR-34a is also elevated in the human failing heart (Thum *et al.*, 2007; Tabuchi *et al.*, 2012). Therapeutic inhibition of miR-34a has been

shown to be beneficial by at least four independent laboratories in cardiac disease models (Bernardo *et al.*, 2012b; Boon *et al.*, 2013; Bernardo *et al.*, 2014a; Huang *et al.*, 2014; Yang *et al.*, 2015). However, in each of these studies, only male mice were examined. To date, the therapeutic potential of silencing miR-34a in females with cardiac pathology has not been explored. Furthermore, the role of miR-34a in models of dilated cardiomyopathy (DCM) and atrial fibrillation (AF) had not previously been assessed. The aim of this study was to examine whether inhibition of miR-34a provides protection in mouse models with DCM and AF, in both males and females.

MATERIAL AND METHODS

Ethical Approval

Animal care and experimentation were conducted in accordance with the Australian code for the care and use of animals for scientific purposes (National Health & Medical Research Council of Australia, 8th Edition, 2013), and approved by the Alfred Medical Research and Education Precinct Animal Ethics Committee. Age- and sex-matched male and female heart disease mice of ~13 weeks of age were euthanised by an i.p. injection of sodium pentobarbital (80 mg/kg). Adequacy of anaesthesia was confirmed by the lack of pedal withdrawal reflex.

Experimental heart disease models

In this study we used two cardiac disease models: 1) a model of moderate dilated cardiomyopathy (referred to as DCM) and 2) a model of more severe DCM with atrial fibrilation (referred to as AF). These models are cardiac-specific transgenic mouse models and were generated as previously described (Pretorius *et al.*, 2009). In brief, mice develop DCM due to transgenic expression of mammalian sterile 20-like kinase 1 (Mst1; (Yamamoto *et al.*, 2003)), and the AF model is generated by mating Mst1 mice with a model with reduced cardiac phosphoinositide 3-kinase (PI3K) activity (due to expression of dominant negative PI3K, dnPI3K; (Shioi *et al.*, 2000)). The Mst1 model is considered clinically relevant because the mice develop DCM as a consequence of increased apoptosis. Male hemizygous Mst1 mice and female hemizygous dnPI3K were bred to generate 1) DCM mice (mice expressing Mst1 alone, Mst1+/-), 2) AF model (mice expressing both Mst1 and dnPI3K i.e. Mst1+/-dnPI3K+/-) and 3) non-transgenic littermate controls (Ntg; Mst1-/-dnPI3K-/-). All mice were littermates, on the same genetic background (C57BL/6-FVB/N). Litters containing the range

of models of both sexes were selected, and mice were body weight-matched before randomly being assigned to treatment. The number of animals per group is as follows: Ntg LNA-control (females N=4, males N=6), Ntg LNA-antimiR-34a (females N=4, males N=5), DCM LNA-control (females N=5, males N=6), DCM LNA-antimiR-34a (females N=8, males N=7), AF LNA-control (females N=4, males N=9), AF LNA-antimiR-34a (females N=5, males N=5). No animals died before the endpoint of the study.

LNA-oligonucleotide synthesis and in vivo delivery

A 15-mer antimiR-34a was synthesised as a LNA:DNA mixmer with a complete phosphorothioate backbone (5'-AgCtaAGacACTgCC-3'; LNA uppercase, DNA lowercase; Roche Innovation Center Copenhagen A/S, Denmark), as previously described (Bernardo *et al.*, 2012b; Bernardo *et al.*, 2014a). The LNA-control sequence (5'-TcAtaCTatAtGaCA-3') is a random sequence designed to have no perfect match binding sites in the transcriptome, and has been validated *in vivo* to not differ from untreated or saline treated animals (Obad *et al.*, 2011; Bernardo *et al.*, 2012b; Bernardo *et al.*, 2014a; Bernardo *et al.*, 2014b; Bernardo *et al.*, 2016). In the current study, there were no differences observed between mice administered LNA-control or saline (data not shown).

At 6-7 weeks of age (after assessment of cardiac function by echocardiography and ECG), mice (Ntg, DCM model, AF model) were randomised to receive a loading dose (25mg/kg subcutaneously) of LNA-control or LNA-antimiR-34a (Monday), 2 subsequent doses at 10mg/kg (Wednesday and Friday), followed by treatment three times per week (10mg/kg subcutaneously; Monday, Wednesday, Friday) for an additional 5 weeks i.e. total treatment period of 6 weeks (Figure 1A). This was followed by a final assessment of cardiac function and ECG prior to tissue collection (measurement of body weight (BW), heart weight (HW), atria weight (AW), lung weight (LW) and tibia length (TL)).

Assessment of left ventricular dimensions and function

Cardiac function was assessed non-invasively before and after treatment by echocardiography (two-dimensional M-mode) in anesthetised mice (1.8% isoflurane) using a Philips iE33 ultrasound machine with a 15MHz linear array transducer. LV wall thickness (LV posterior wall, LVPW), LV chamber dimensions (LV end-diastolic dimension, LVEDD; LV end-systolic dimension, LVESD), heart rate (HR) and fractional shortening (FS; [(LVEDD-LVESD)/LVEDD] x 100%) were measured from the short axis view. All measurements were

performed with an off-line analysis system (ProSolv Cardiovascular Analyzer 3.5; ProSolv) from at least 3 beats that were averaged. Prior to treatment, cardiac function was comparable in the DCM groups of the same gender (e.g. male DCM LNA-control vs. male DCM LNA-antimiR-34a) and AF groups (data not shown).

Cardiac conduction by ECG

Direct ECGs were recorded from anaesthetised mice (1.8% isoflurane) by placing a pair of 27G needle electrodes subcutaneously (right arm and chest lead equivalent to V5). Signals were sampled for at least 5 min using the Powerlab system and BioAmp (ADInstruments, Australia). ECG parameters (PR, RR, P and R-amplitudes, HR) were measured using Chart 5 (ECG analysis module). Since the shape of P waves can be abnormal in the DCM and AF models (making detection by the ECG analysis module difficult), PR intervals were also confirmed manually.

Histological analyses

Ventricle samples were fixed in 4% paraformaldehyde, dehydrated and embedded in paraffin. Cardiac collagen deposition/interstitial fibrosis was assessed by Masson's trichrome stain (Alfred Pathology, Melbourne, Australia). Images of the LV were obtained using an Olympus light microscope at 40x magnification. Collagen stained blue, which was measured and analyzed using Image-Pro Analyzer version 7.0. The percentage fibrosis was calculated by dividing the total area of collagen by the total area of the LV and multiplying by 100%. Photos of whole hearts were taken for visualisation of cardiac chambers.

RNA extraction and mRNA gene expression analyses

Total RNA was extracted from mouse ventricles using TRI-reagent (Sigma Aldrich, St. Louis, MI, USA). For mRNA Northern blotting, 20μg of total RNA was electrophoresed in a 1.3% denaturing formaldehyde agarose gel in 1 x MOPS, and transferred onto Hybond N membranes (GE Healthcare, Waukesha, WI). Membranes were blocked in hybridisation solution (50% deionised formamide, 6X SSC, 5X Denhardt's solution, 0.5% SDS) containing 1mg/ml denatured salmon sperm DNA at 42°C for 1h prior to hybridisation. Radiolabeled probes ([α-^{32}P]dCTP) were prepared using a Prime-a-Gene Labeling System (Promega, Madison, WI). Membranes were hybridised with denatured radiolabelled probes at 42ºC overnight (2 x 10^6 cpm/ml of hybridisation solution). Membranes were rinsed twice at room

temperature in 2X SSC, twice at 42ºC in 2X SSC/1% SDS for 5 min, and twice in 0.1X SSC for 30 min. Amersham Hyperfilm MP autoradiography films (GE Healthcare) were exposed to membranes with an intensifying screen at -80°C. Membranes were probed for B-type natriuretic peptide (*Nppb*/Bnp) and collagen 3 (*Col3a1*), and glyceraldehyde-3-phosphate dehydrogenase (*Gapdh*).

miRNA expression

For Northern blotting, 15µg of total RNA was electrophoresed in a 20% TBE acrylamide gel using High-density TBE sample buffer and transferred to Amersham Hybond™-N+ nylon membrane (GE Healthcare) by electrophoresis. The membrane was cross-linked in a UV-crosslinker, pre-hybridized (45°C for 30 min in ULTRAhyb®-Oligo Hybridization Buffer, Life Technologies, Carlsbad, CA), and probed with LNA-modified oligonucleotides (Exiqon, Denmark), complementary to mature miRNA-34a and sno-U6 (used as a loading control). 10pmol of each LNA oligonucleotide was end-labelled with [γ-32P]ATP (Perkin Elmer, Waltham, MA) by using T4 polynucleotide kinase (New England Biolabs, Ipswich, MA) for 1 hour at 37°C. Hybridisation with labeled probes (5 min at 100°C prior to addition) was conducted at 45°C overnight in ULTRAhyb®-Oligo Hybridization Buffer (Life Technologies). After hybridisation, the membranes were washed for 30 min in NorthernMax® Low Stringency Wash Buffer (Life Technologies) at 45°C, high stringency wash in 0.5X SSC for 30 min at 45°C (for LNA-oligonucleotide miR-34a) or 0.1X SSC for 30 min at 45°C (for LNA-oligonucleotide sno-U6). The membranes were exposed using autoradiography film.

For qPCR analysis, 2µg of total RNA was DNAse treated with Ambion's TURBO DNA-free kit (Life Technologies) according to the manufacturer's recommendations. To detect the level of miR-27a, miR-34a, miR-34b and miR-34c, RT-qPCR was performed using TaqMan® MicroRNA Assays (Life Technologies) using 50ng total RNA on an Applied Biosystems Quant Studio 6 and 7 real-time PCR instrument (Life Technologies). Expression was normalised against snoU6 using the $2^{-\Delta\Delta Ct}$ method of quantification.

MiRNA-Seq for miRNA expression analysis

Two samples from the following groups were used for miRNA-Seq: male Ntg control (1 saline treated mouse, 1 LNA-control), female Ntg control (2 LNA-control), male DCM control (2 LNA-control), male DCM antimiR-34a (2 LNA-antimiR-34a), female DCM

control (2 LNA-control), female DCM antimiR-34a (2 LNA-antimiR-34a), male AF control (2 LNA-control), male AF antimiR-34a (2 LNA-antimiR-34a), female AF control (2 LNA-control), female AF antimiR-34a (2 LNA-antimiR-34a).

Standard miRNA-Seq libraries were prepared as described by the manufacturer's instructions (Illumina). Samples (24 per lane) were multiplexed and sequenced on the Illumina Genome Analyzer HiSeq 2000 (read length: 50bp, Ramaciotti Centre for Genomics, University of NSW). MiRNA-Seq reads were aligned to the mouse reference genome (mm10) using Partek Flow®; version 3.0 (Partek Inc.) with default settings unless otherwise indicated. After removing adaptor sequences, the bases of unaligned reads were trimmed for a minimum Phred quality score of 20 (default settings used except minimum read length=17). Fastq files were then aligned to the mm10 reference genome with Bowtie 1 (default parameters used except seed mismatch limit=0, seed length=22, alignments reported per read=10) and Bowtie 2 (default parameters except interval between seeds S,1,1.25, ambiguous characters function L,O.15, default reporting mode=false, max alignments reported per read=10; http://bowtie-bio.sourceforge.net/index.shtml (Langmead *et al.*, 2009)). Prealignment and postalignment quality control was performed, and read counts were filtered for reads with minimum mapping quality of 20 (99% of reads met this criteria). The trimmed, aligned and filtered data were quantitated to known miRNAs using miRBase mature miRNA database (version 21, released 3rd July, 2014). Reads are presented as log2 transcript counts from miRNA sequencing normalised to reads per kilobase of transcript per million mapped reads (RPKM)(Partek Genomics Suite®, version 6.6). For comparisons between the 2 Ntg groups, a t-test was performed. For comparisons between the 4 DCM/AF groups a one-way analysis of variance (ANOVA) was performed. Unadjusted P-values are presented in Supplementary Tables S3-S5. Heat maps were generated using the MeV software (v4.8.1 TIGR MultiExperiment Viewer, http://www.tm4.org) with the specific parameters (t-test based on Welch approximation, P-value based on t-distribution and hierarchical clustering using Pearson correlation) (Saeed *et al.*, 2003).

Statistical analysis

Results are presented as mean±S.E.M. All statistics were performed using StatView and GraphPad Prism software v.6.02, unless otherwise indicated. Differences between groups were identified using one-way ANOVA followed by Fisher least significant difference post hoc pairwise tests (when the ANOVA was significant). Unpaired t tests were used when

comparing 2 groups for a single measure. For small animal groups (n=4) in which data was not normally distributed, differences between groups were identified using a Mann Whitney non-parametric t-test. A value of $P<0.05$ was considered significant. All relative units are expressed as a fold change with the relevant control group normalised to 1.

RESULTS

miR-34a levels are elevated in the DCM and AF cardiac disease models and inhibited by LNA-antimiR-34a

Tissue was harvested from mice 6 weeks after commencing treatment with LNA-antimiR-34a or LNA-control (Figure 1A). miR-34a expression levels were increased in the hearts of the female DCM and AF models compared with Ntg (Figure 1B; see LNA-control groups). A similar observation was made in the male disease models, though miR-34a was only significantly elevated in the hearts of the male AF model compared with Ntg (Figure 1B). Administration of LNA-antimiR-34a significantly reduced miR-34a levels in both males and females (Figure 1B). Inhibition of miR-34a was confirmed in a subset of samples by Northern blotting (Figure 1C). The presence of the shifted miR-34a:LNA-antimiR-34a band (duplex) on the Northern blot indicates that LNA-antimiR-34a has sequestered miR-34a in a stable heteroduplex, inhibiting its function, as previously reported (Bernardo *et al.*, 2012b).

Inhibition of miR-34a is more effective attenuating DCM-induced morphological changes in female mice than male mice

Prior to administration of LNA-antimiR-34a or LNA-control, the DCM and AF models displayed cardiac dysfunction, atrial enlargement, and ECG abnormalities (Figure 2A and 2B; arrhythmia also present in the AF model). At tissue dissection (6 weeks after LNA-antimiR-34a/control), the DCM and AF models were associated with dilatation of LV chambers and thinning of ventricular walls (Figure 2C). Female DCM mice displayed heart enlargement compared with Ntg controls (Figure 3A), and this was accompanied by atrial enlargement and increased lung weights (both markers of a failing heart) (Figures 3B and 3C, Table 1). Male DCM mice also had increased heart weights, atria weights and lung weights compared with Ntg controls (Figure 3A-C, Table 2), however, the percent increases in males were generally more modest than that observed in females (e.g. HW/TL increased ~33% in females and 9% in males). LNA-antimiR-34a treatment prevented significant increases in normalized heart, atria and lung weights in the DCM female model (Figure 3A-C, Table 1).

Whilst LNA-antimiR-34a also prevented significant increases in normalised heart and lung weights in the DCM male model, it had no effect on atrial weight (Figure 3A-C, Table 2). The AF model was also associated with increased atrial and lung weights (Figure 3B and 3C). Treatment with LNA-antimiR-34a was not associated with significant improvements in cardiac morphology or lung weights in female and male AF mice (Figure 3, Table 1 and Table 2).

Inhibition of miR-34a was associated with better cardiac function in the DCM model but not the AF model

Hearts of the DCM and AF models display cardiac dilatation, thinning of the ventricular walls and a fall in cardiac function (assessed by calculating FS). The models are also associated with ECG abnormalities. On the majority of parameters, abnormalities in cardiac dimensions, function and ECG parameters, are more severe in the AF model than the DCM model (see LNA-control groups for Ntg, DCM, AF, Tables 3-6). Administration of LNA-antimiR-34a for 6 weeks was associated with more favorable cardiac function and LV wall thickness in female mice as compared to female DCM mice administered LNA-control (Figure 4A and 4B, Table 3). Cardiac function also tended to be greater in LNA-antimiR-34a treated male DCM mice compared with LNA-control male DCM mice, but this was not statistically significant. There was also no notable improvement in other echocardiography parameters (Table 4). LNA-antimiR-34a provided no benefit in the AF model of either sex (Figure 4A and 4B, Tables 3 and 4). ECG parameters were not significantly changed by LNA-antimiR-34a in the disease models (Tables 5 and 6).

LNA-antimiR-34a induced protection in the female DCM model is associated with an improved cardiac molecular profile

The DCM and AF models have previously been shown to be associated with increased expression of cardiac stress and collagen genes; which are likely to contribute to cardiac dysfunction and conduction abnormalities (Pretorius *et al.*, 2009; Sapra *et al.*, 2014). In the current study, BNP and collagen 3 gene expression levels were elevated in the hearts of both male and female DCM and more significantly in AF mice (Figure 5A-B; see LNA-control groups). BNP was elevated less in LNA-antimiR-34a treated female DCM hearts than LNA-control female DCM hearts (Figure 5A). Collagen 3 gene expression was lower in LNA-antimiR-34a treated female DCM mice than LNA-control female DCM mice (Figure 5B).

Consistent with this finding, LNA-antimIR-34a treated female DCM mice displayed less cardiac fibrosis than LNA-control female DCM mice (Figure 5C). Inhibition of miR-34a had no effect on gene expression in any other group (Figure 5A-B).

Sex- and treatment-dependent regulation of miRNAs in the diseased heart

To assess whether differential expression of other miRNAs might contribute to the phenotype of male and female DCM and AF models, we examined the expression of other miR-34 family members (miR-34b and miR-34c) by qPCR, as well as other miRNAs by miRNA-Seq. Expression of miR-34b and miR-34c were previously shown to be elevated in other cardiac disease settings and contribute to cardiac pathology (Bernardo *et al.*, 2012b). Furthermore, while miR-34 family members share some common targets, miR-34b and miR-34c are also predicted to target genes which are distinct from miR-34a (Supplementary Figure S1, Supplementary Tables S1 and S2). Cardiac expression levels of miR-34b and miR-34c were generally higher in the DCM and AF models of both sexes (Figure 6A and 6B). However, there were no distinct differences related to sex or disease model which are likely to explain why LNA-antimiR-34a treatment provided more protection in the female DCM model, and no protection in the AF model.

By miRNA-Seq, the expression levels of miRNAs in hearts from normal adult mice which have been characterized as cardiac specific/selective were comparable in both sexes (Ntg; Figure 7A e.g. miR-133a-3p, miR-208a-3p). Interestingly, there was distinct regulation of less well characterised miRNAs in male and female Ntg hearts (Figure 7B, Supplementary Table S3). Next, we interrogated miRNAs in the DCM and AF models with and without LNA-antimiR-34a treatment. Presentation of differentially expressed miRNAs in heatmaps highlighted the distinct regulation of some miRNAs between sexes in the disease models, as well as with LNA-antimiR-34a treatment (Figures 7C and 7D, Supplementary Table S4 and S5). Expression of 3 miRNAs in Figure 7 have been validated by qPCR (Supplementary Figure S2).

DISCUSSION

Despite numerous studies examining the role of miRNAs in settings of cardiac disease, and the development of miRNA-based therapies, very little is known about whether these disease-induced miRNAs are regulated similarly in both sexes (Sharma & Eghbali, 2014). This study represents the first to examine the effect of silencing miR-34a in the female heart. To our

knowledge, it also represents the only report which has specifically compared the effect of inhibiting any miRNA in the adult heart in both sexes. Results from this study highlight the need to characterise the expression of miRNAs in both males and females, and in different cardiac disease settings. This information will be critical for determining which patient groups are most likely to respond favourably to therapeutic interventions.

There were three major new findings to come from the current study. First, inhibition of miR-34a provided more protection in the female DCM model than the male DCM model. Second, silencing miR-34a provided no significant benefit in the more severe model of DCM associated with AF in either males or females. Third, we identified miRNAs which were differentially regulated in the diseased heart of males and females, and some of these were differentially affected by LNA-antimiR-34a treatment. Collectively, these finding have important implications for the development of miRNA-based therapies for heart disease.

In the current study, we assessed the potential of attenuating expression of miR-34a in a model of DCM with moderate cardiac pathology and dysfunction, and a more severe model of DCM also associated with cardiac conduction abnormalities including AF (referred to as the AF model). LNA-antimiR-34a treatment was able to provide some benefit in the DCM model in both males and females, but interestingly, the therapeutic intervention was more effective in females than males. This could be explained, at least in part, due to miR-34a playing a more dominant role in the DCM-induced phenotype in females than males. Consistent with this hypothesis, the fold increase in miR-34a expression levels in the female DCM heart compared with Ntg were higher than those found in the male DCM heart.

The AF model is a more severe model than the DCM model, characterised by more dilatation of cardiac chambers, higher expression of cardiac stress genes and more severe cardiac conduction abnormalities (Pretorius *et al.*, 2009). Even though miR-34a was elevated in the hearts of the AF model in both sexes, silencing miR-34a provided no protection against cardiac pathology and dysfunction. The therapeutic benefit of inhibiting miR-34a in the moderate DCM model, but not the more severe DCM model with AF is consistent with our previous report, in which LNA-antimiR-34a provided protection in a setting of moderate pressure overload but not severe pressure overload (Bernardo *et al.*, 2014a). In a more severe setting, additional miRNAs are likely to be dysregulated. Thus, it may be necessary to target a group of miRNAs concurrently rather than a single miRNA (Bernardo *et al.*, 2012b; Bernardo *et al.*, 2014a).

To further explore why LNA-antimiR-34a administration may have been more effective in the female DCM model that then male DCM model, and why the treatment was ineffective in the AF model, we undertook some additional experiments. First, we assessed the expression of other miR-34 family members which have also been associated with cardiac pathology. In mammals, the miR-34 family consists of three homologous transcripts miR-34a, miR-34b and miR-34c. In the mouse, miR-34a is located on chromosome 4, while miR-34b/c are located on chromosome 9. In humans, the miR-34a gene maps to chromosome 1p36.22, whereas the genes coding for both miR-34b and miR-34c map to chromosome 11q23.1 (Agostini & Knight, 2014). Expression levels of miR-34b and miR-34c were elevated in the hearts of the DCM and AF models, as previously shown in other cardiac stress models (pressure overload and MI; higher expression in more severe cardiac stress settings (Bernardo *et al.*, 2012b; Bernardo *et al.*, 2014a)). However, there were no notable differences in expression of miR-34b and miR-34c between sexes in the DCM model which are likely to contribute to the better outcome in LNA-antimiR-34a treated female DCM mice. Furthermore, even though the AF model is a more severe model than the DCM model, miR-34b and miR-34c were expressed at comparable levels in the two models. Thus, heightened expression of miR-34b and miR-34c are unlikely to account for the differences observed. Next, we performed miRNA-Seq to examine the global expression of all miRNAs in the diseased models with and without LNA-antimiR-34a. To our knowledge, a direct comparison of miRNAs regulated in the female and male adult heart in cardiac disease settings, together with a therapeutic intervention, has not previously been reported. Murphy and colleagues profiled 609 miRNAs in hearts from 15 week adult male and female C57BL/6J mice under basal conditions using an Affymetrix miRNA microarray (Evangelista *et al.*, 2013). Eight miRNAs were identified to be differentially regulated in the heart between the sexes; 4 miRNAs had higher relative expression in males than females (miR-144, miR-34b-3p, miR-205, miR-222), and 4 miRNAs had higher relative expression in females (miR-1, miR-106b, miR-720, miR-29b) (Evangelista *et al.*, 2013). In another study, expression of miR-1 was found to be expressed at lower levels in female but not male adult rat ventricular myocytes following stimulation with a pathological stimulus, phenylephrine (no significant differences were observed in unstimulated control myocytes) (Stauffer *et al.*, 2011). A more recent study examined tissue and sex associated miRNAs in zebrafish under basal settings (Vaz *et al.*, 2015). Sex-associated miRNAs were identified in brain and liver; hearts from male and female zebrafish were not specifically examined (Vaz *et al.*, 2015). Regitz-Zagrosek and

colleagues examined the expression of a group of miRNAs (miR-21, -24, -27a, -27b, -106a, -106b) in hearts of male and female mice with pathological hypertrophy due to pressure overload induced by aortic constriction (Queiros *et al.*, 2013). Each of these miRNAs was more highly expressed in the hypertrophied male heart than the female heart. In humans, previous studies have identified miRNAs which are dysregulated in the heart or circulation in cardiac disease settings (Thum *et al.*, 2007; Devaux *et al.*, 2013; Matsumoto *et al.*, 2013). However, these studies have not specifically examined sex differences in miRNA expression, or were heavily biased towards male subjects. In our study, miRNA-Seq analyses demonstrated that a number of miRNAs were differentially expressed in the male and female DCM and AF models, and LNA-antimiR-34a differentially regulated some of these miRNAs. The underlying mechanisms responsible for this finding will require further studies. However, it is noteworthy that sex steroid hormones and X-linked genes can influence the regulation of miRNAs (Sharma & Eghbali, 2014), and oestradiol can regulate miR-34a (Li *et al.*, 2014). Furthermore, while LNA-antimiR-34a directly targets miR-34a specifically (Bernardo *et al.*, 2012b), because miR-34a regulates the expression of numerous target genes including transcription factors (which can regulate other miRNAs), and due to feedback loops, other miRNAs can be differentially regulated as a "secondary" response (Matkovich *et al.*, 2013; Ooi *et al.*, 2016). Altogether, this highlights the differential regulation and complexity of miRNA-drug interactions in the male and female heart.

It is important to acknowledge that no animal model will perfectly mimic human disease, and differences in species need to be considered (Riley *et al.*, 2012). For instance, the high heart rate and small atrial size of mice compared with humans are factors which contribute to the absence of permanent AF in mice. The disease animal models used in the current study (DCM and AF) were selected because they display some characteristics which are similar to human cardiac disease (e.g. left ventricular dilation, fibrosis, lung congestion, molecular changes observed in human diseased hearts) (Yamamoto *et al.*, 2003; Pretorius *et al.*, 2009; Sapra *et al.*, 2014). Furthermore, the genetic alterations in the hearts of the mouse models (i.e. increased Mst1 and decreased PI3K) are also features which have been observed in human DCM and AF (Pretorius *et al.*, 2009; Maejima *et al.*, 2013).

The success of miRNA therapeutics in preclinical models of disease has led to the development and translation of miRNA therapies into the clinic for hepatitis C virus (Janssen *et al.*, 2013) and liver cancer (Bader, 2012). miRNA-based therapies have also shown

potential in preclinical models of cardiac pathology but are yet to enter the clinic for cardiovascular disease. One of the biggest steps for translation of a miRNA based therapy for heart failure is identifying strategies for specific and efficient delivery to the heart (see reviews (Ooi *et al.*, 2014; Bernardo *et al.*, 2015)). Nonetheless, with improvements and developments with delivery tools (including the use of nanoparticles, liposomes and antibodies), miRNA-based therapies remain a promising approach for the treatment of heart failure (Bernardo *et al.*, 2015).

In conclusion, the current study contributes to the growing body of literature showing that inhibition of miR-34a represents a promising therapeutic approach in a number of cardiac disease settings (Bernardo *et al.*, 2012b; Boon *et al.*, 2013; Bernardo *et al.*, 2014a; Huang *et al.*, 2014; Yang *et al.*, 2015). However, the lack of benefit in the more severe DCM model with AF, is also consistent with previous work showing that silencing miR-34a is less effective in settings of severe cardiac pathology (Bernardo *et al.*, 2012b; Bernardo *et al.*, 2014a). The present study also uncovered differential responses of the male and female heart to LNA-antimiR-34a treatment in a setting of DCM. Our subsequent identification of sex-, disease- and treatment-regulated miRNAs has important and broad implications for the development of miRNA-based therapies for cardiovascular disease, and potentially others diseases.

AUTHOR CONTRIBUTION

Experiments were performed in the Cardiac Hypertrophy Research Laboratory at Baker IDI Heart and Diabetes Institute. JRM and BCB contributed to experimental design and coordinated the project; RCYL contributed to experimental design and coordinated the miRNA-Seq experiment; BCB, JYYO, AM, YKT, SS, NLP, HK, RCYL and JRM contributed to acquisition, analysis or interpretation of data; SO contributed to experimental design and provided the LNA-antimiRs, JS provided the Mst1 Tg model and expertise regarding this model; JRM and BCB wrote the paper. All authors approved the manuscript final version and agreed to be accountable for all aspects of the work in ensuring that questions related to the accuracy or integrity of any part of the work were appropriately investigated and resolved. All persons designated as authors qualify for authorship, and all those who qualify for authorship are listed.

ACKNOWLEDGEMENTS

We thank Geeta Sapra for ECG assistance and Nicole Jennings for assistance with echocardiography.

FUNDING

This study was funded by National Health and Medical Research Council Project Grant 586603 (to JRM and RCYL), and also supported in part by the Victorian Government's Operational Infrastructure Support Program. JRM is a National Health and Medical Research Council Senior Research Fellow (586604 & 1078985). JRM and RCYL were also supported by an Australian Research Council Future Fellowship (FT0001657), and a University of New South Wales Vice Chancellor Research Fellowship, respectively.

Conflict of interest statement: SO is an employee of Roche Innovation Center Copenhagen A/S, a clinical-stage biopharmaceutical company that develops RNA-targeted therapeutics.

SUPPORTING INFORMATION

Supplementary Figure S1: Predicted targets of the miR-34 family members.

Supplementary Figure S2: Validation of miR-seq data by qPCR.

Supplementary Figure S3: Heat map of mmu-miR-34a-5p.

Supplementary Table S1: Predicted mRNA targets to miR-34a, but not miR-34b and miR-34c.

Supplementary Table S2: Predicted mRNA targets common to both miR-34b and miR-34c.

Supplementary Table S3: List of cardiac specific/selective miRNAs and differentially expressed miRNAs in hearts from male and female Ntg mice from miR-seq data.

Supplementary Table S4: List of differentially expressed miRNAs in hearts from male and female DCM mice with LNA-control or LNA-antimiR-34a from miR-seq data.

Supplementary Table S5: List of differentially expressed miRNAs in hearts from male and female AF mice with LNA-control or LNA-antimiR-34a from miR-seq data.

REFERENCES

Agostini M & Knight RA. (2014). miR-34: from bench to bedside. *Oncotarget* **5,** 872-881.

Bader AG. (2012). miR-34 - a microRNA replacement therapy is headed to the clinic. *Front Genet* **3,** 120.

Bernardo BC, Charchar FJ, Lin RC & McMullen JR. (2012a). A MicroRNA Guide for Clinicians and Basic Scientists: Background and Experimental Techniques. *Heart Lung Circ* **21,** 131-142.

Bernardo BC, Gao XM, Tham YK, Kiriazis H, Winbanks CE, Ooi JY, Boey EJ, Obad S, Kauppinen S, Gregorevic P, Du XJ, Lin RC & McMullen JR. (2014a). Silencing of miR-34a attenuates cardiac dysfunction in a setting of moderate, but not severe, hypertrophic cardiomyopathy. *PLoS ONE* **9,** e90337.

Bernardo BC, Gao XM, Winbanks CE, Boey EJ, Tham YK, Kiriazis H, Gregorevic P, Obad S, Kauppinen S, Du XJ, Lin RC & McMullen JR. (2012b). Therapeutic inhibition of the miR-34 family attenuates pathological cardiac remodeling and improves heart function. *Proc Natl Acad Sci U S A* **109,** 17615-17620.

Bernardo BC, Nguyen SS, Gao XM, Tham YK, Ooi JY, Patterson NL, Kiriazis H, Su Y, Thomas CJ, Lin RC, Du XJ & McMullen JR. (2016). Inhibition of miR-154 Protects Against Cardiac Dysfunction and Fibrosis in a Mouse Model of Pressure Overload. *Sci Rep* **6,** 22442.

Bernardo BC, Nguyen SS, Winbanks CE, Gao XM, Boey EJ, Tham YK, Kiriazis H, Ooi JY, Porrello ER, Igoor S, Thomas CJ, Gregorevic P, Lin RC, Du XJ & McMullen JR. (2014b). Therapeutic silencing of miR-652 restores heart function and attenuates adverse remodeling in a setting of established pathological hypertrophy. *FASEB J* **28,** 5097-5110.

Bernardo BC, Ooi JY, Lin RC & McMullen JR. (2015). miRNA therapeutics: a new class of drugs with potential therapeutic applications in the heart. *Future Med Chem* **7,** 1771-1792.

Bernardo BC, Weeks KL, Pretorius L & McMullen JR. (2010). Molecular distinction between physiological and pathological cardiac hypertrophy: experimental findings and therapeutic strategies. *Pharmacol Ther* **128,** 191-227.

Boon RA, Iekushi K, Lechner S, Seeger T, Fischer A, Heydt S, Kaluza D, Treguer K, Carmona G, Bonauer A, Horrevoets AJ, Didier N, Girmatsion Z, Biliczki P, Ehrlich JR, Katus HA, Muller OJ, Potente M, Zeiher AM, Hermeking H & Dimmeler S. (2013). MicroRNA-34a regulates cardiac ageing and function. *Nature* **495,** 107-110.

Devaux Y, Vausort M, McCann GP, Kelly D, Collignon O, Ng LL, Wagner DR & Squire IB. (2013). A panel of 4 microRNAs facilitates the prediction of left ventricular contractility after acute myocardial infarction. *PLoS ONE* **8,** e70644.

Editorial. (2010). Putting gender on the agenda. *Nature* **465,** 665.

Evangelista AM, Deschamps AM, Liu D, Raghavachari N & Murphy E. (2013). miR-222 contributes to sex-dimorphic cardiac eNOS expression via ets-1. *Physiol Genomics* **45,** 493-498.

Hata A. (2013). Functions of microRNAs in cardiovascular biology and disease. *Annu Rev Physiol* **75,** 69-93.

Huang Y, Qi Y, Du JQ & Zhang DF. (2014). MicroRNA-34a regulates cardiac fibrosis after myocardial infarction by targeting Smad4. *Expert Opin Ther Targets* **18,** 1355-1365.

Janssen HL, Reesink HW, Lawitz EJ, Zeuzem S, Rodriguez-Torres M, Patel K, van der Meer AJ, Patick AK, Chen A, Zhou Y, Persson R, King BD, Kauppinen S, Levin AA & Hodges MR. (2013). Treatment of HCV infection by targeting microRNA. *N Engl J Med* **368,** 1685-1694.

Kim AM, Tingen CM & Woodruff TK. (2010). Sex bias in trials and treatment must end. *Nature* **465,** 688-689.

Langmead B, Trapnell C, Pop M & Salzberg SL. (2009). Ultrafast and memory-efficient alignment of short DNA sequences to the human genome. *Genome Biol* **10,** R25.

Legato MJ. (2016). Gender-specific medicine in the genomic era. *Clin Sci (Lond)* **130,** 1-7.

Li XJ, Ren ZJ & Tang JH. (2014). MicroRNA-34a: a potential therapeutic target in human cancer. *Cell Death Dis* **5,** e1327.

Maejima Y, Kyoi S, Zhai P, Liu T, Li H, Ivessa A, Sciarretta S, Del Re DP, Zablocki DK, Hsu CP, Lim DS, Isobe M & Sadoshima J. (2013). Mst1 inhibits autophagy by promoting the interaction between Beclin1 and Bcl-2. *Nat Med* **19,** 1478-1488.

Matkovich SJ, Hu Y & Dorn GW, 2nd. (2013). Regulation of cardiac microRNAs by cardiac microRNAs. *Circ Res* **113,** 62-71.

Matsumoto S, Sakata Y, Suna S, Nakatani D, Usami M, Hara M, Kitamura T, Hamasaki T, Nanto S, Kawahara Y & Komuro I. (2013). Circulating p53-responsive microRNAs are predictive indicators of heart failure after acute myocardial infarction. *Circ Res* **113,** 322-326.

Obad S, dos Santos CO, Petri A, Heidenblad M, Broom O, Ruse C, Fu C, Lindow M, Stenvang J, Straarup EM, Hansen HF, Koch T, Pappin D, Hannon GJ & Kauppinen S. (2011). Silencing of microRNA families by seed-targeting tiny LNAs. *Nat Genet* **43,** 371-378.

Ooi JY, Bernardo BC & McMullen JR. (2014). The therapeutic potential of miRNAs regulated in settings of physiological cardiac hypertrophy. *Future Med Chem* **6,** 205-222.

Ooi JY, Bernardo BC, Singla S, Patterson NL, Lin RC & McMullen JR. (2016). Identification of miR-34 regulatory networks in settings of disease and antimiR-therapy: Implications for treating cardiac pathology and other diseases. *RNA Biol***,** April 28.0. E-pub ahead of print. PMID: 27124358.

Pretorius L, Du XJ, Woodcock EA, Kiriazis H, Lin RC, Marasco S, Medcalf RL, Ming Z, Head GA, Tan JW, Cemerlang N, Sadoshima J, Shioi T, Izumo S, Lukoshkova EV, Dart AM, Jennings GL & McMullen JR. (2009). Reduced phosphoinositide 3-kinase (p110alpha) activation increases the susceptibility to atrial fibrillation. *Am J Pathol* **175,** 998-1009.

Queiros AM, Eschen C, Fliegner D, Kararigas G, Dworatzek E, Westphal C, Sanchez Ruderisch H & Regitz-Zagrosek V. (2013). Sex- and estrogen-dependent regulation of a miRNA network in the healthy and hypertrophied heart. *Int J Cardiol* **169,** 331-338.

Rathore SS, Wang Y & Krumholz HM. (2002). Sex-based differences in the effect of digoxin for the treatment of heart failure. *N Engl J Med* **347,** 1403-1411.

Regitz-Zagrosek V. (2006). Therapeutic implications of the gender-specific aspects of cardiovascular disease. *Nat Rev Drug Discov* **5,** 425-438.

Riley G, Syeda F, Kirchhof P & Fabritz L. (2012). An introduction to murine models of atrial fibrillation. *Front Physiol* **3,** 296.

Saeed AI, Sharov V, White J, Li J, Liang W, Bhagabati N, Braisted J, Klapa M, Currier T, Thiagarajan M, Sturn A, Snuffin M, Rezantsev A, Popov D, Ryltsov A, Kostukovich E, Borisovsky I, Liu Z, Vinsavich A, Trush V & Quackenbush J. (2003). TM4: a free, open-source system for microarray data management and analysis. *Biotechniques* **34,** 374-378.

Sapra G, Tham YK, Cemerlang N, Matsumoto A, Kiriazis H, Bernardo BC, Henstridge DC, Ooi JY, Pretorius L, Boey EJ, Lim L, Sadoshima J, Meikle PJ, Mellet NA, Woodcock EA, Marasco S, Ueyama T, Du XJ, Febbraio MA & McMullen JR. (2014). The small-molecule BGP-15 protects against heart failure and atrial fibrillation in mice. *Nat Commun* **5,** 5705.

Sharma S & Eghbali M. (2014). Influence of sex differences on microRNA gene regulation in disease. *Biol Sex Differ* **5,** 3.

Shioi T, Kang PM, Douglas PS, Hampe J, Yballe CM, Lawitts J, Cantley LC & Izumo S. (2000). The conserved phosphoinositide 3-kinase pathway determines heart size in mice. *EMBO J* **19,** 2537-2548.

Stauffer BL, Sobus RD & Sucharov CC. (2011). Sex differences in cardiomyocyte connexin43 expression. *J Cardiovasc Pharmacol* **58,** 32-39.

Tabuchi T, Satoh M, Itoh T & Nakamura M. (2012). MicroRNA-34a regulates the longevity-associated protein SIRT1 in coronary artery disease: effect of statins on SIRT1 and microRNA-34a expression. *Clin Sci* **123,** 161-171.

Thum T, Galuppo P, Wolf C, Fiedler J, Kneitz S, van Laake LW, Doevendans PA, Mummery CL, Borlak J, Haverich A, Gross C, Engelhardt S, Ertl G & Bauersachs J. (2007). MicroRNAs in the Human Heart: A Clue to Fetal Gene Reprogramming in Heart Failure. *Circulation* **116,** 258-267.

Vaz C, Wee CW, Lee GP, Ingham PW, Tanavde V & Mathavan S. (2015). Deep sequencing of small RNA facilitates tissue and sex associated microRNA discovery in zebrafish. *BMC Genomics* **16,** 950.

Yamamoto S, Yang G, Zablocki D, Liu J, Hong C, Kim SJ, Soler S, Odashima M, Thaisz J, Yehia G, Molina CA, Yatani A, Vatner DE, Vatner SF & Sadoshima J. (2003). Activation of Mst1 causes dilated cardiomyopathy by stimulating apoptosis without compensatory ventricular myocyte hypertrophy. *J Clin Invest* **111,** 1463-1474.

Yang Y, Cheng HW, Qiu Y, Dupee D, Noonan M, Lin YD, Fisch S, Unno K, Sereti KI & Liao R. (2015). MicroRNA-34a Plays a Key Role in Cardiac Repair and Regeneration Following Myocardial Infarction. *Circ Res* **117,** 450-459.

Figure 1. miR-34a is elevated in the heart in a setting of DCM and AF, and silenced with LNA-antimiR-34a. (A) Experimental time line. **(B)** Quantification of miR-34a relative to snoU6 by qPCR. Data are expressed as mean ± SEM. Ntg: n=4-5/group, DCM: n=4-6/group, AF: n=4-9/group. **P*<0.05 vs. LNA-control of the same group; †*P*<0.05 vs. Ntg LNA-control. 1 Way ANOVA with Fisher's post hoc test. **(C)** Northern blot of miR-34a and snoU6 in hearts of Ntg, DCM and AF 6 weeks post administration with LNA-control (con) or LNA-antimiR-34a (anti).

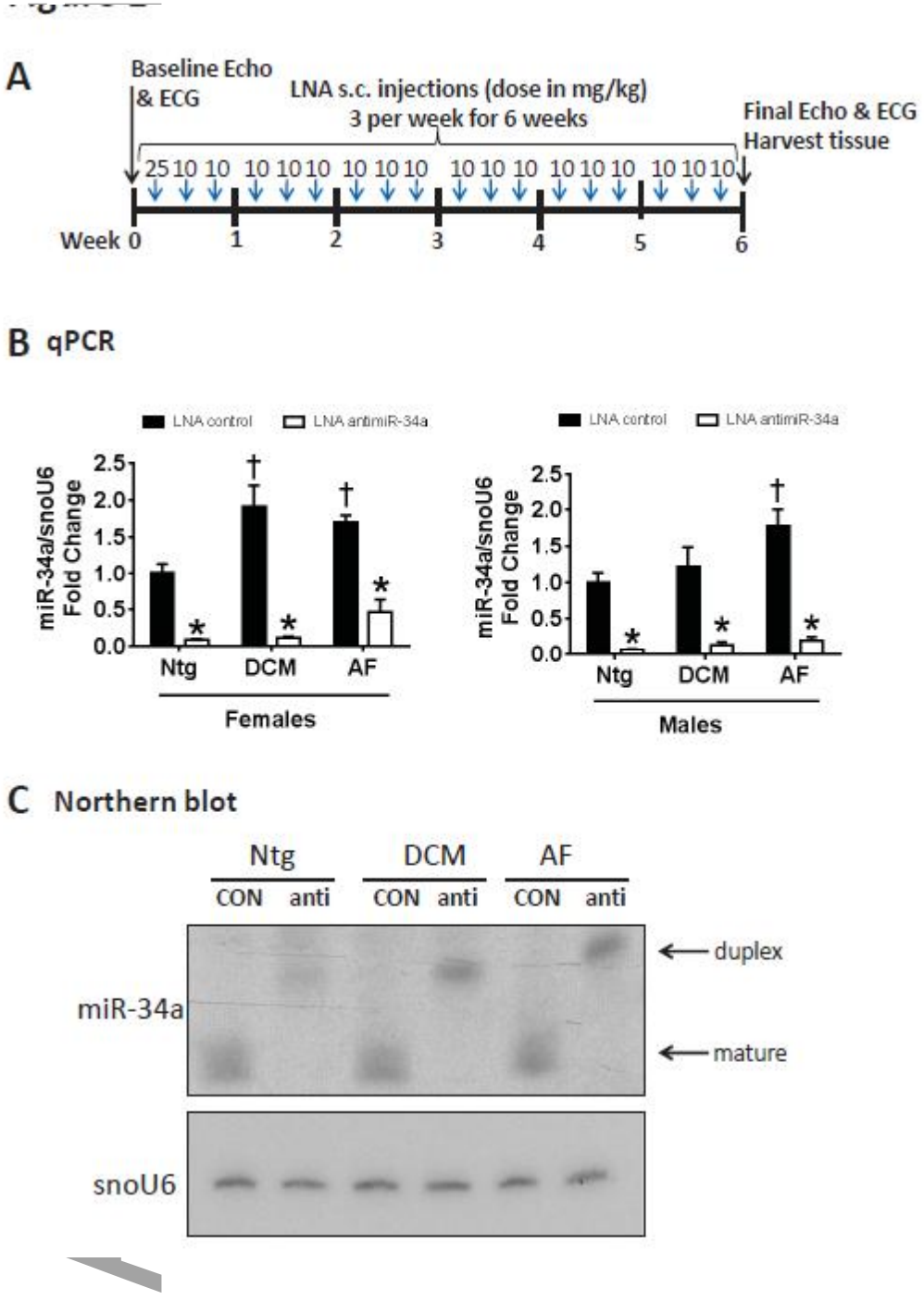

Figure 2. The DCM and AF models are associated with cardiac dysfunction, ECG abnormalities and dilatation of cardiac chambers. (A) Representative echocardiography images (upper panels, m-mode; lower panels, long axis view highlighting differences in left atrial size, LA) and **(B)** ECG traces of Ntg, DCM and AF mice prior to treatment. Dots on the ECG traces are positioned above the R waves and highlight the irregular rhythm of the AF model. Red arrows highlight P-waves. **(C)** Transverse sections of hearts highlighting dilated chambers in the female and male DCM and AF models. LV=left ventricle, RV=right ventricle. Scale bar = 1 mm.

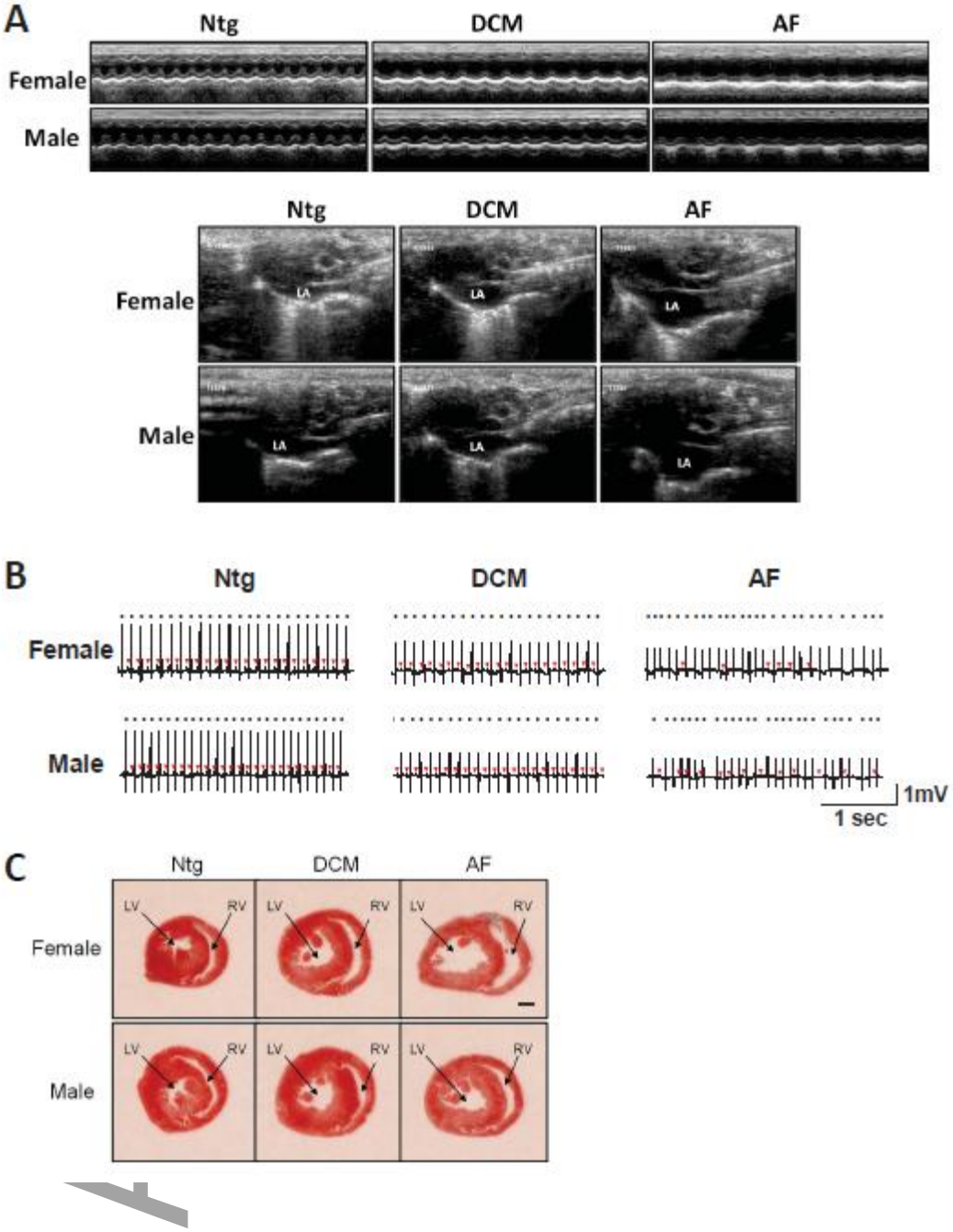

Figure 3. Inhibition of miR-34a improves cardiac morphology more in female DCM mice than male DCM mice. Graphs of **(A)** heart weight/tibia length (HW/TL), **(B)** atria weight/TL (AW/TL) and **(C)** lung weight/TL (LW/TL) in female and male Ntg, DCM and AF mice. Data are expressed as mean ± SEM. Female Ntg: n=4/group, female DCM: n=5-8/group, female AF: n=4-5/group. Male Ntg: n=5-6/group, male DCM: n=6-7/group, male AF: n=5-9/group. **P*<0.05 vs. Ntg of same treatment group, †*P*<0.05 (1 Way ANOVA with Fisher's post hoc test of Ntg, DCM and AF groups), ^*P*<0.05 vs. Ntg of same treatment group (unpaired t test), #*P*<0.05 (1 Way ANOVA with Fisher's post hoc test of Ntg and DCM groups only), P=0.057 (Mann Whitney non-parametric t-test).

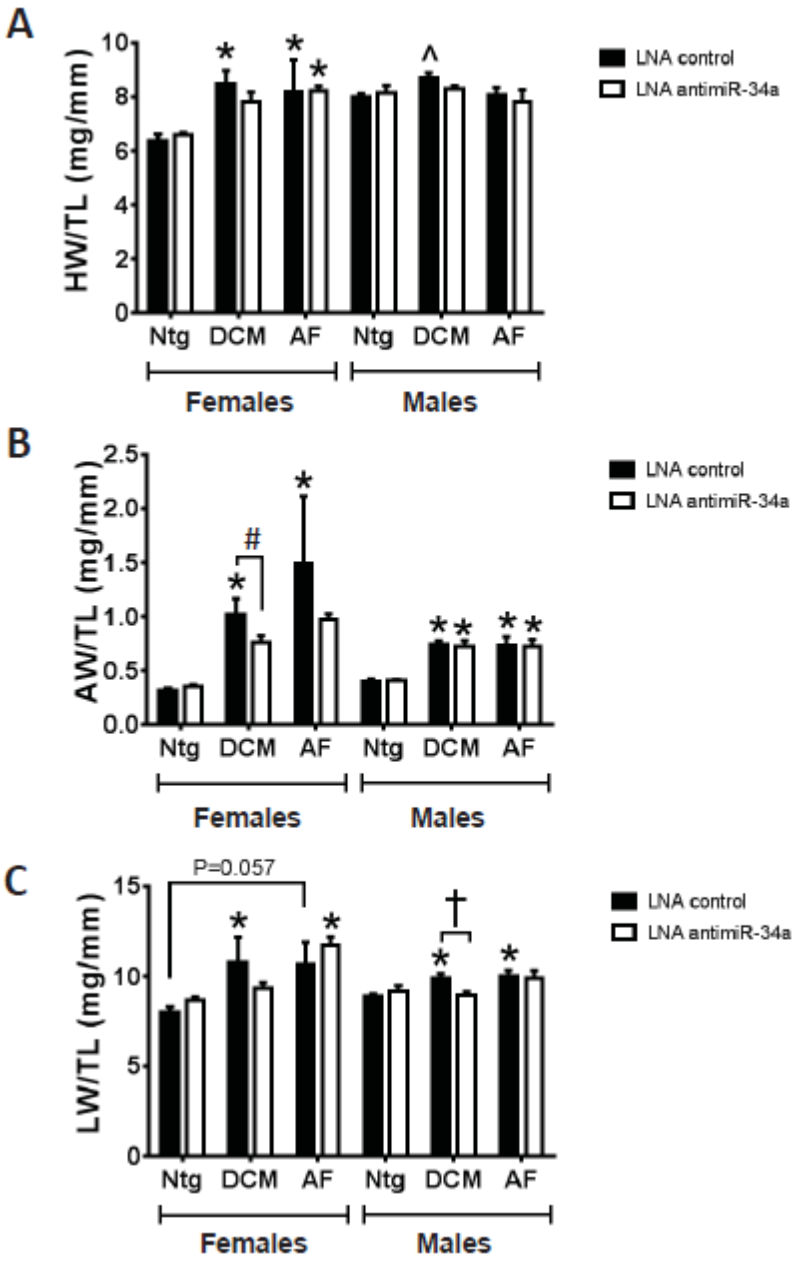

Figure 4. Administration of LNA-antimiR-34a is associated with better cardiac function in the DCM model, but not the AF model. Quantification of **(A)** fractional shortening and **(B)** left ventricular posterior wall thickness (LVPW) 6 weeks post-treatment. Mean ± SEM. Ntg n=4/group, DCM n=5-7/group, AF n=4-5/group. **P*<0.05 vs. Ntg of same treatment, †*P*<0.05 vs. LNA-control of same model, ‡*P*<0.05 vs. DCM of same treatment (1 Way ANOVA with Fisher's post hoc test of Ntg, DCM and AF groups). P=0.064 (Mann Whitney non-parametric t-test).

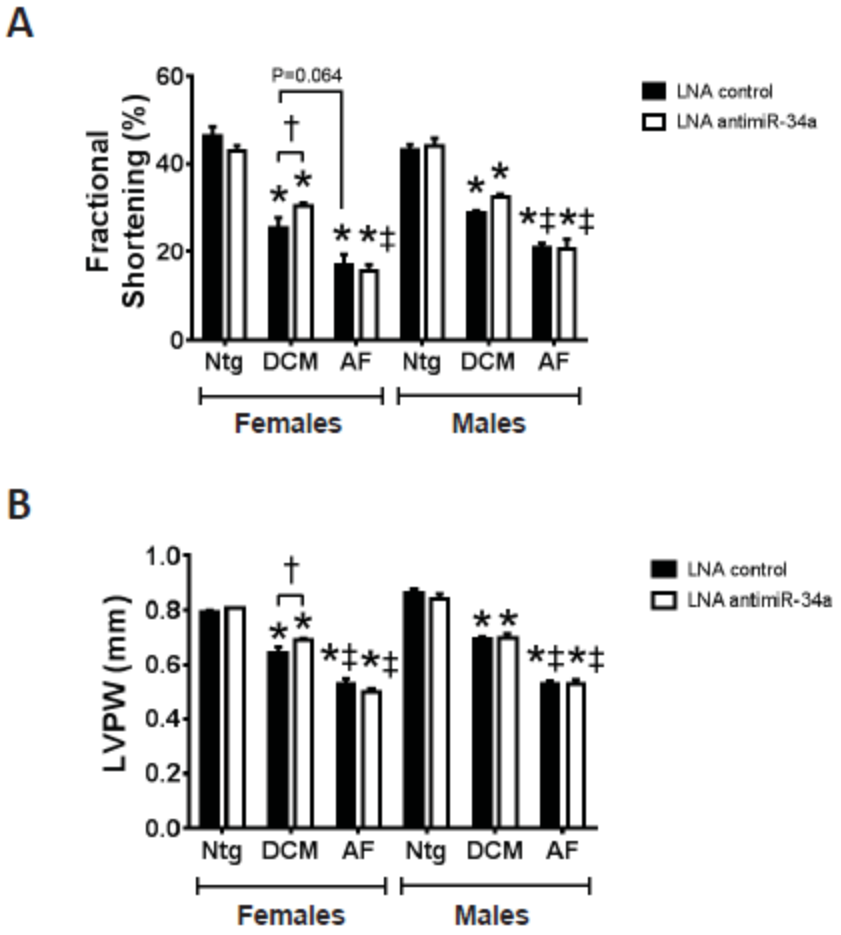

Figure 5. LNA-antimiR-34a treatment is associated with a more favorable cardiac molecular profile in female DCM mice but not male DCM mice. (A) Quantification of BNP (*Nppb*) and **(B)** collagen 3 (*Col3a1*) relative to *Gapdh* in hearts of female and male Ntg, DCM and AF LNA-control and LNA-antimiR-34a treated mice. Mean ± SEM. Ntg: n=3-4/group, DCM: n=4-6/group, AF: n=4-5/group. **P*<0.05 ***P*<0.005, ****P*<0.001 vs. Ntg of same treatment group (1 Way ANOVA with Fisher's post hoc test of Ntg, DCM and AF groups). †*P*<0.05 (1 Way ANOVA with Fisher's post hoc test of Ntg and DCM groups only). **(C)** LV cross-sections stained with Masson's trichrome and quantification of LV fibrosis in female DCM LNA control and LNA antimiR-34a treated hearts. n=4/group. *P<0.05 (unpaired t-test). Scale bar=200μM.

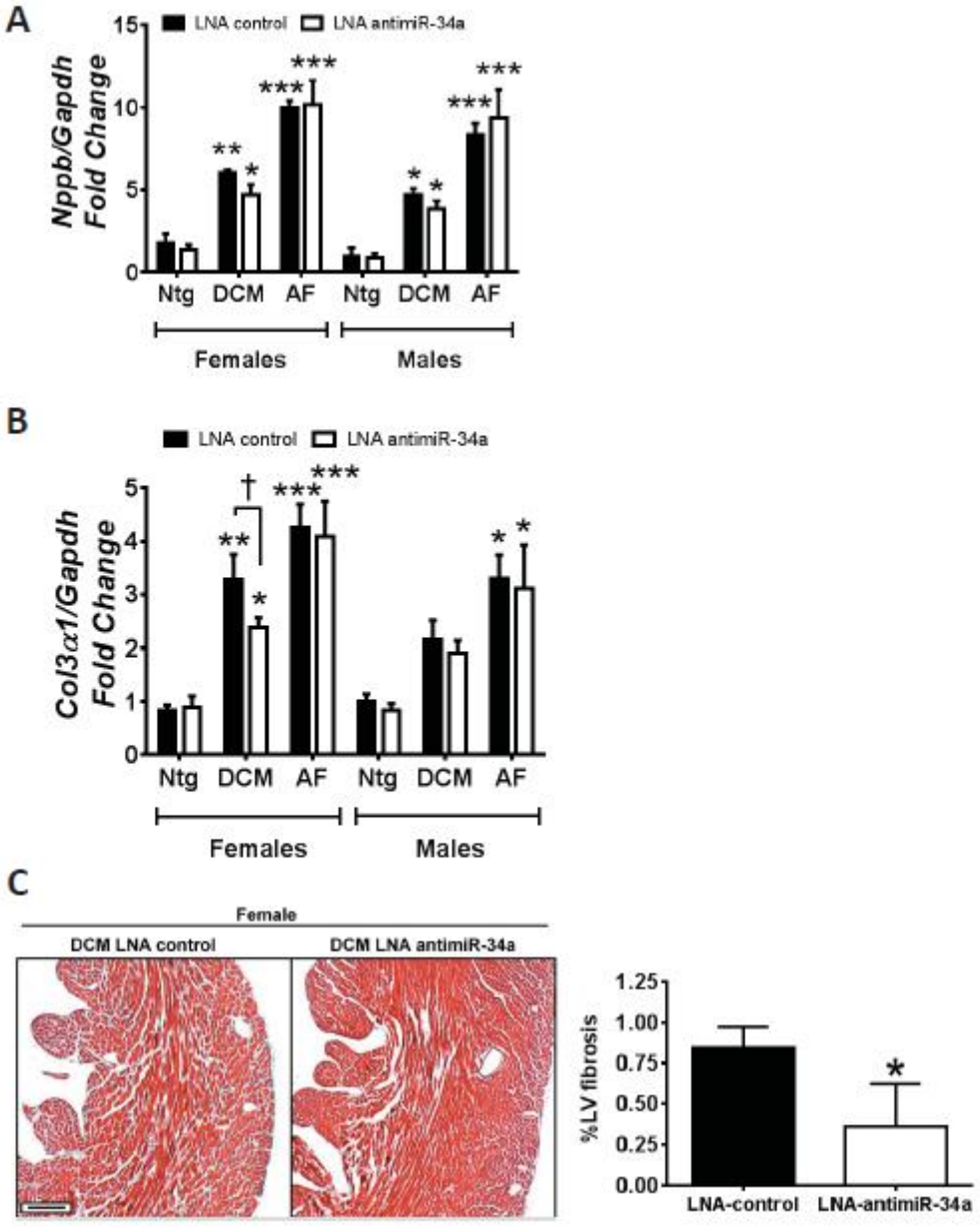

Figure 6. Expression of miRNA-34b and miRNA-34c are elevated in the DCM and AF models. Quantification of **(A)** miR-34b and **(B)** miR-34c relative to snoU6 by qPCR in LNA-control hearts. Data are expressed as mean ± SEM. The Ntg group for females and males has been normalized to 1.0. Ntg: n=4/group, DCM: n=3-5/group, AF: n=4-5/group. *$P \leq 0.05$ vs. Ntg, $P=0.06$. Unpaired t-test.

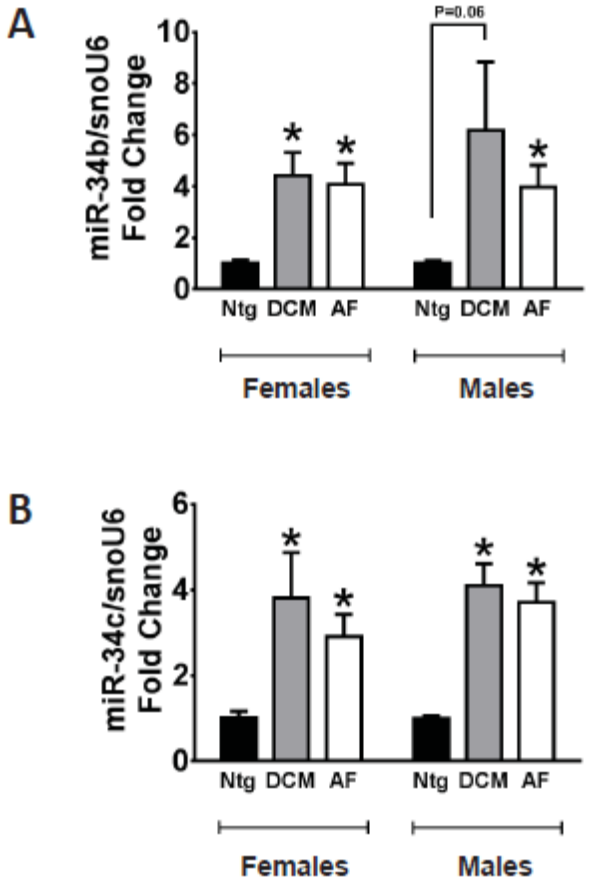

Figure 7. Sex- and treatment-dependent regulation of miRNAs in the diseased heart. Expression of **(A)** cardiac specific/selective miRNAs and **(B)** differentially expressed miRNAs in hearts from male and female Ntg mice (control). No differentially expressed miRNAs identified in panel A). Differentially expressed miRNAs in hearts from male and female DCM mice **(C)** and AF mice **(D)** with LNA-control or LNA-antimiR-34a. Each row represents a miRNA and each column represents an individual heart sample. Yellow represents upregulation in comparison to male Ntg control and blue represents downregulation. N.B. Sex differences in the expression of miR-34a-5p in the DCM model (Fig 7C) are difficult to visualise in this heatmap because a scale was selected to encompass the wide variation in expression of numerous miRNAs within the DCM model. An additional heat map with a scale optimised for miR-34a-5p and a comparison of Ntg with DCM is provided in Supplementary Figure S4. This visualisation is consistent with the sex difference in miR-34a in the DCM model presented in Figure 1B.

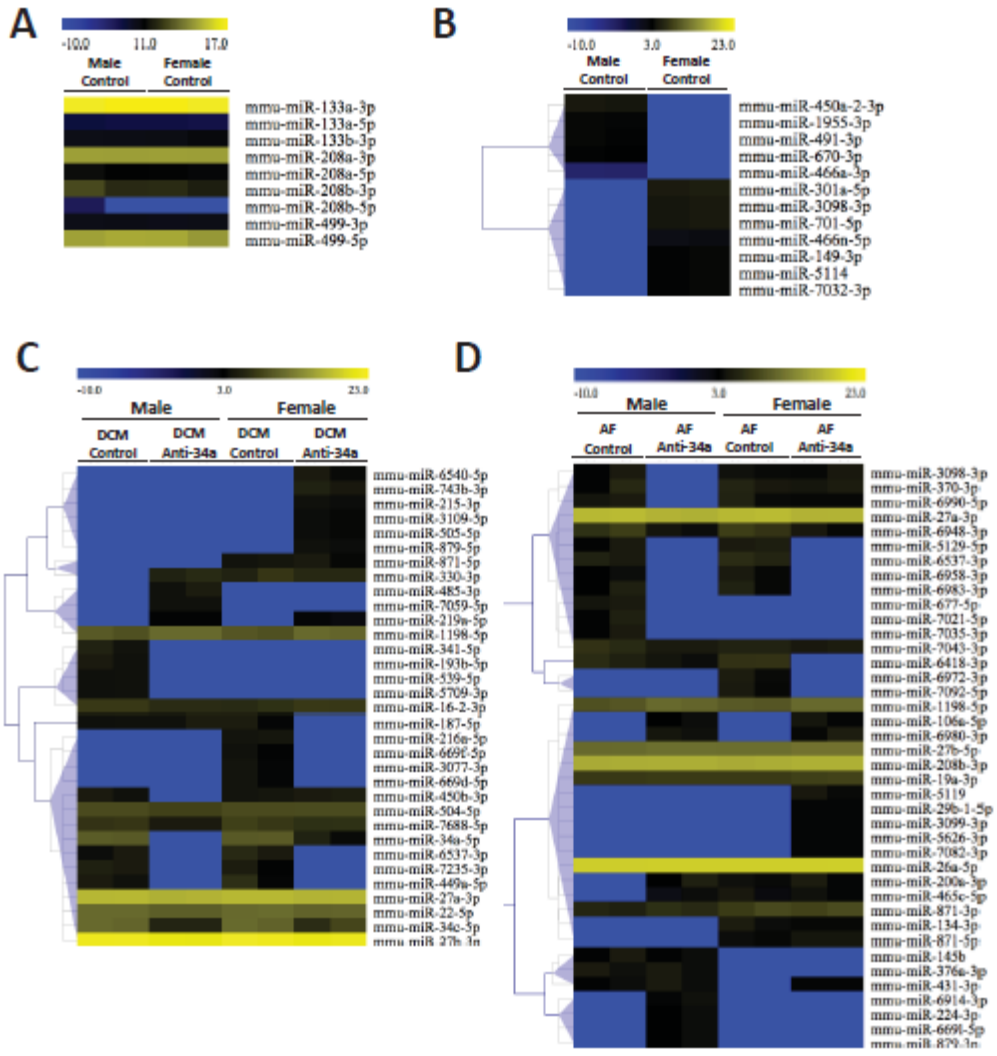

Table 1. Morphological data of Ntg, DCM and AF LNA-control and LNA-antimiR-34a female mice following 6 weeks of treatment.

FEMALES	Ntg		DCM		
	LNA-control	LNA-antimiR-34a	LNA-control	LNA-antimiR-34a	LNA-contro
No. of animals	4	4	5	8	4
Age (weeks)	13.2 ± 0.4	14.0 ± 0.9	13.1 ± 0.6	12.4 ± 0.5	12.9 ± 0.5
Body weight (g)	24.1 ± 0.8	24.9 ± 0.5	26.0 ± 1.0	25.5 ± 0.7	25.2 ± 1.1
Tibial length (mm)	16.7 ± 0.1	16.7 ± 0.1	16.4 ± 0.3	16.6 ± 0.1	16.7 ± 0.2
HW (mg)	106.7 ± 3.6	110.4 ± 1.6	138.5 ± 8.3*	130.4 ± 7.0	136.8 ± 20
AW (mg)	5.3 ± 0.4	5.9 ± 0.3	16.7 ± 2.5*	12.6 ± 1.3	25.0 ± 10
LW (mg)	133.7 ± 3.9	144.6 ± 3.2	176.6 ± 24.2*	155.4 ± 6.8	177.8 ± 21
HW/TL (mg/mm)	6.4 ± 0.2	6.6 ± 0.1	8.5 ± 0.5*	7.8 ± 0.4	8.2 ± 1.2
AW/TL (mg/mm)	0.31 ± 0.02	0.35 ± 0.02	1.02 ± 0.15*	0.75 ± 0.07	1.49 ± 0.6
LW/TL (mg/mm)	8.0 ± 0.3	8.7 ± 0.2	10.8 ± 1.4*	9.3 ± 0.3	10.7 ± 1.2

BW, body weight; TL, tibial length; HW, heart weight; AW, atrial weight; LW, lung weight. Data are shown as mean ± SEM. *P<0.05 vs. Ntg of the same treatment. One Way ANOVA with Fisher's post-hoc test. ‖P=0.057 vs. Ntg of same treatment (Mann Whitney non-parametric t-test).

Table 2. Morphological data of Ntg, DCM and AF LNA-control and LNA-antimiR-34a male mice following 6 weeks of treatment.

MALES	Ntg		DCM		
	LNA-control	LNA-antimiR-34a	LNA-control	LNA-antimiR-34a	LNA-control
No. of animals	6	5	6	7	9
Age (weeks)	13.6 ± 0.6	13.6 ± 0.7	13.3 ± 0.5	13.6 ± 0.5	13.7 ± 0.3
Body weight (g)	32.6 ± 1.0	31.7 ± 1.0	32.3 ± 0.5	31.7 ± 0.6	32.6 ± 0.6
Tibia length (mm)	16.6 ± 0.1	16.8 ± 0.1	16.9 ± 0.1	16.8 ± 0.1	16.8 ± 0.2
HW (mg)	132.9 ± 3.0	136.6 ± 4.8	146.8 ± 3.4	139.9 ± 2.0	135.6 ± 4.0
AW (mg)	6.7 ± 0.4	6.9 ± 0.2	12.5 ± 0.7*	12.1 ± 0.9*	12.2 ± 1.4*
LW (mg)	147.6 ± 1.7	154.2 ± 5.2	166.5 ± 4.7*	150.8 ± 3.2†	168.0 ± 5.2*
HW/TL (mg/mm)	8.0 ± 0.1	8.1 ± 0.3	8.7 ± 0.2^	8.3 ± 0.1	8.1 ± 0.3
AW/TL (mg/mm)	0.40 ± 0.02	0.41 ± 0.01	0.74 ± 0.04*	0.72 ± 0.05*	0.73 ± 0.09
LW/TL (mg/mm)	8.9 ± 0.1	9.2 ± 0.3	9.9 ± 0.3*	9.0 ± 0.2†	10.0 ± 0.3*

BW, body weight; TL, tibia length; HW, heart weight; AW, atrial weight; LW, lung weight. Data are shown as mean ± SEM. One Way ANOVA with Fisher's post-hoc test. *P<0.05 vs. Ntg of the same treatment, ^P<0.05 vs. Ntg of the same treatment (unpaired t test), †P<0.05 vs. DCM LNA-control.

Table 3. Echocardiography measurements in Ntg, DCM and AF LNA-control and LNA-antimiR-34a female mice six weeks post-treatment.

FEMALES	Ntg		DCM		
	LNA-control	LNA-antimiR-34a	LNA-control	LNA-antimiR-34a	LNA-contr
No. of animals	4	4	5	7	4
HR, bpm	622 ± 22	628 ± 12	578 ± 14	524 ± 26	515 ± 44
LVPW, mm	0.80 ± 0.01	0.81 ± 0.00	0.65 ± 0.02*	0.69 ± 0.01*†	0.53 ± 0.02
LVEDD, mm	3.76 ± 0.02	3.76 ± 0.07	4.28 ± 0.17*	4.29 ± 0.10*	4.66 ± 0.29
LVESD, mm	2.01 ± 0.08	2.14 ± 0.03	3.20 ± 0.23*	2.99 ± 0.09*	3.89 ± 0.35
FS, %	46 ± 2	43 ± 1	26 ± 2*	30 ± 1*†	17 ± 2*‖

HR, heart rate; LV, left ventricular; LVPW, LV posterior wall thickness; LVEDD, LV end-diastolic dimension; LVESD, LV end-systolic dimension; FS, fractional shortening. Data are shown as mean ± SEM. *P<0.05 vs. Ntg of same treatment, †P<0.05 vs. LNA-control of same model, ‡P<0.05 vs. DCM of same treatment. One Way ANOVA with Fisher's post-hoc test. ‖P=0.063 vs. DCM of same treatment (Mann Whitney non-parametric t-test).

Table 4. Echocardiography measurements in Ntg, DCM and AF LNA-control and LNA-antimiR-34a male mice six weeks post-treatment

MALES	Ntg		DCM		
	LNA-control	LNA-antimiR-34a	LNA-control	LNA-antimiR-34a	LNA-cont
No. of animals	5	5	6	7	9
HR, bpm	588 ± 16	609 ± 22	560 ± 21	562 ± 20	597 ± 19
LVPW, mm	0.86 ± 0.02	0.84 ± 0.02	0.69 ± 0.01*	0.70 ± 0.02*	0.53 ± 0.0
LVEDD, mm	4.04 ± 0.05	3.81 ± 0.16	4.45 ± 0.09*	4.19 ± 0.10*	4.63 ± 0.0
LVESD, mm	2.29 ± 0.03	2.13 ± 0.13	3.17 ± 0.06*	2.82 ± 0.08* (†P=0.06)	3.67 ± 0.1
FS, %	43 ± 1	44 ± 2	29 ± 1*	33 ± 1* † P=0.06	21 ± 1*

HR, heart rate; LV, left ventricular; LVPW, LV posterior wall thickness; LVEDD, LV end-diastolic dimension; LVESD, LV end-systolic dimension; FS, fractional shortening. Data are shown as mean ± SEM. One Way ANOVA with Fisher's post-hoc test. **P*<0.05 vs. Ntg of same treatment, †*P*=0.06 vs. LNA-control of same model, ‡*P*<0.05 vs. DCM of same treatment.

Table 5: Electrocardiography measurements in Ntg, DCM and AF LNA-control and LNA-antimiR-34a female mice six weeks post-treatment

FEMALES	Ntg		DCM		
	LNA-control	LNA-antimiR-34a	LNA-control	LNA-antimiR-34a	L
No. of animals	3	3	4	5	
HR, bpm	581 ± 9	534 ± 3	520 ± 16	509 ± 17	53
RR, ms	104 ± 2	112 ± 1	116 ± 4	120 ± 4	11
PR, ms	34 ± 1	36 ± 1	49 ± 1*	51 ± 3*	5
R amplitude (mV)	1.64 ± 0.13	1.77 ± 0.08	1.17 ± 0.11*	1.13 ± 0.12*	0.9

Data are shown as mean ± SEM. One Way ANOVA with Fisher's post-hoc test. *P<0.05 vs. Ntg of same treatment, †P<0.05 vs. LNA-control of same model.

This is the author manuscript accepted for publication and has undergone full peer review but has not been through the copyediting, typesetting, pagination and proofreading process, which may lead to differences between this version and the Version of Record. Please cite this article as doi: 10.1113/JP272512.

Table 6: Electrocardiography measurements in Ntg, DCM and AF LNA-control and LNA-antimiR-34a male mice six weeks post-treatment

MALES	Ntg		DCM		
	LNA-control	LNA-antimiR-34a	LNA-control	LNA-antimiR-34a	LN
No. of animals	5	5	4	4	
HR, bpm	569 ± 7	574 ± 16	572 ± 2	538 ± 28	54
RR, ms	106 ± 1	105 ± 3	105 ± 0	113 ± 6	11
PR, ms	33 ± 1	34 ± 1	44 ± 2*	43 ± 1*	5
R amplitude, mV	1.63 ± 0.08	1.70 ± 0.08	1.11 ± 0.05*	1.22 ± 0.08*	0.9

Data are shown as mean ± SEM. One Way ANOVA with Fisher's post-hoc test. *P<0.05 vs. Ntg of same treatment, ‡P<0.05 vs. DCM of same treatment.